CHARACTERIZATION OF Nd: YAG LASER RADIATION EFFECTS ON Ti6Al4V PHYSICO-CHEMICAL PROPERTIES: AN IN VIVO STUDY

J. Tavakoli, M. E. Khosroshahi* and M. Mahmoodi

Biomaterial Group, Faculty of Biomedical Engineering
Amirkabir University of Technology, Tehran, Iran
khosro@aut.ac.ir

*Corresponding Author

(Received: Febuary 24, 2006 - Accepted: March 18, 2007)

Abstract The effect of a Nd: YAG laser (1064 nm) has been studied on Ti6Al4V alloy in terms of optical and physical parameters for biomedical applications. The superior surface microhardness hardness (i.e. 377 VHN) is attributed to grain refinement associated with laser melting and rapid solidification. The electrochemical property, mainly pitting corrosion resistance, has been carried out in Hanks salt balanced physiological solution using standard potentiodynamic polarization testing. At the optimium laser treating fluence (140 Jcm^{-2}), the EDX spectroscopy showed a decrease of about 30 % in the vanadium and the contact angle measurements also indicated an improved surface wettability seen in the characteristics with a contact angle of 35°. Finally, Cell spreading on the implanted specimens was analyzed by SEM and their condition in a specific area was studied for 10 cells for three separate regions on the same specimen using Image J Program software. The *in vivo* tests provided some useful clinical and pathological information regarding tissue response to the implants with different surface topography.

Keywords Ti Alloy, Nd: YAG Laser, Corrosion, Contact Angle, Surface Micro Hardness, Cell Adhesion

چکیده در این مقاله تاثیر برهمکنش لیزر Nd: YAG بر آلیاژ تیتانیوم بر حسب پارامترهای اپتیکی – فیزیکی مورد بررسی قرار گرفت. مطالعات نشان داد که با استفاده از لیزر در شرایط بهینه (140 $J.cm^{-2}$)، دست یابی به آلیاژ با خواص فیزیکی و شیمیایی مناسب و همچنین زیست سازگار میسر می‌باشد. افزایش مقاومت خوردگی، کاهش وانادیوم در سطح، کاهش زاویه تماس، افزایش سختی سطح در اثر تابش لیزر به سطح از جمله نتایجی است که در این مطالعه بدست آمد. مطا لعات حیوانی (*in vivo*) نشان داد که چسبندگی سلولهای استخوانی به سطح برای نمونه اصلا ح شده با لیزر در شرایط بهینه نسبت به نمونه شاهد افزایش می‌یابد.

1. INTRODUCTION

Biomaterials designed for permanent bone and joint replacement need to have suitable physical and mechanical properties and acceptable biocompatibility. In orthopaedic and dentistry, metals like stainless steel, cobalt chromium alloys, titanium and titanium alloys are widely used. The greatest disadvantages of steel, besides the high stiffness leading to stress shielding beneath osteosynthesis plates, is its high corrosion rate, resulting in the release of adverse ions like nickel and chromium into the surrounding tissues [1-3]. The elements cobalt and chromium alloys have been demonstrated to be toxic for cells [4].

Titanium has an excellent biocompatibility due to the fact that it is highly inert and insoluble in body fluids and forms a protective oxide layer on the surface [5]. However, pure titanium could leave metal debris in the tissue due to the higher tendency to produce wear in fretting conditions. Therefore, numerous titanium alloys like Ti6Al4V, with improved physical and mechanical properties have been developed [6]. Ti6Al4V alloy has become one of the most practical biomaterials due to its excellent corrosion resistance, acceptable

mechanical properties and low toxicity [7]. Its module of elasticity and strength is 5.6 and 6 folding greater than bone, respectively. In addition to chemistry, however, the surface topography of the Ti6Al4V is important. Surfaces are treated to facilitate an intimate contact between bone and implant. So, the tissue response to an implant involves physical factors, depending on implant design, surface topography, surface charge density, surface free energy and chemical factors associated with the composition of the materials. These substrate characteristics may directly influence cell adhesion, spreading and signaling, events that regulate a wide variety of biological functions [8].

Ion implantation [9], coating [10], sand blast [11] and machining are some of the most commonly used techniques to change implant surface topography, however, laser treatment is going to play an important role in this field [12-16]. This fact is related to its wavelength selectivity, photon coherency, very low thermal or mechanical damage, high accuracy, control and less pollution during laser treatment processes. In fact, optical and kinetics of laser parameters like fluence and pulse number as well as surface physical parameters will affect this process.

In our study, Nd: YAG laser radiation effects on corrosion resistance, surface chemical composition, microhardness, surface wettability and cell adhesion on Ti6Al4V surface will be analyzed. In addition, animal implantation approach is considered to evaluate osteoblast cells adhesivity to implant surfaces after laser treatment.

2 .MATERIALS AND METHOD

2.1. Sample Preparation Rectangular-shaped specimens with 20 × 10 mm dimensions and the thickness of 2 mm, were made from a medical grade Ti6Al4V (ASTM F136, Friadent GmbH,Mannheim, Germany) with chemical formulation Ti (91.63 %) Al (5.12 %) V (3.25 %). The samples were divided into two groups of control and laser treated samples. All samples were cleaned with 97 % ethanol and subsequently were washed twice with distilled water in an ultrasonic bath (Mattachanna, Spain). A final rinse with deionized water at neutral pH was performed to ensure a clean surface.

2.2. Laser Setup Surface treatment was conducted by a Nd: YAG laser with 200 μs pulse Maximum average output power and energy per pulse were adjustable up to 45 W and 50 J/pulse, respectively. All experiments were carried out at 1 Hz frequency. In order to achieve optimum surface treatment conditions, melting and evaporation thresholds and variations of etch depth versus fluence were evaluated. Laser scanning velocity was kept constant by a precise adjustable xyz translator.

2.3. Surface Analysis and Tests All the laser surface treatment experiments were performed under ambient conditions. Surface morphology, chemical composition of the untreated and laser treated specimens were analyzed by SEM and EDXA. The surface energy of the samples were determined by measuring the contact angle (θ) (Kruss-G40-instrument)of test liquids (diiodo-Methane and water; Busscher) on the titanium plates and plots of the Ownes-Wendt-Kaeble's equation:

$$\gamma_{lv}(1+\cos\theta) = 2(\gamma_l^d.\gamma_s^d)^{0.5} + 2(\gamma_l^p.\gamma_s^p)^{0.5} \quad (1)$$

Where s and l represent solid and liquid surfaces respectively, γ^d stands for the dispersion component of the total surface energy (γ) and γ^p is the polar component.

Scanning electron microscopy (stereoscan 360, Cambridge Instrument Company) as well as the adhered cell spreading and morphology were used to examine the surface topography of modified titanium samples. The standard Tofel polarization test was carried out to study the corrosion behaviour of specimens in Hank's physiological solution at 37ºC. The metal corrosion behaviour was studied by measuring the current and plotting the E-logI diagram. Surface microhardness test was carried out with 50 gram load in 10 seconds by a diamond square tip. Each related test considered at 5 points and reported as an average. Surface energy and contact angle measurements were performed by Wu method in order to evaluate the surface wettability after laser treatment.

2.4. Animal Implantation one untreated and

two laser treated specimens were implanted in a leg on the upper part of femur bone of an eight month male goat weighing 30 Kg. Specimens were steam sterilized before implantation in an autoclave (Mattachnna, Barcelona-Spain). The steam sterilization was conducted under 132°C, 2 bar and in 45 minutes. All the specimens were labeled by separate codes using an engraver, for further studies. The operation site was shaved and depilated with soft soap and ethanol before surgery, the site was also disinfected with 70 % ethanol and was covered with a sterile blanket. In order to proceed with the implantation, cortex bone was scraped by osteotom (Medeicon®, Tuttlingen-Germany) after cutting the limb from one-third end in lateral side and elevating it by a self-retaining retractor. A copious physiological saline solution irrigation was used during implantation to prevent from over heating. To ensure a stable passive fixation of implants during the healing period, they were stabilized by size 4 and 8 titanium wires (Atila ortoped®, Tehran-Iran) without any external compression forces.

After the operation the animal was protected from infection by proper doses of Penicillin and Gentamicine for a period of eight days. Then it was returned to its ordinary life situation. After six months the animal was killed and the specimens were removed.

2.5. Cell Analysis cell growth in the implanted specimens was analyzed by SEM. The cell spreading situation and area was studied by Image J Program software. The number of attached cells was calculated by a coulter counter using enzyme detachment method and Trypsin-EDTA (0.025 V/V) in PBS media. The final amount of attached cell can be studied by plotting cell detachment rate versus time.

2.6. Histopathology Following implantation, the specimens with their surrounding tissues were retrieved and prepared for histological evaluation. The specimens' related tissues were fixed in 4 % formalin solution (pH = 7.3), dehydrated in a graded series of ethanol (10 %, 30 %, 50 %, 70 % and 90 %) and embedded in paraffin after decalcification. Then, 10 µm thick slices were prepared per specimens using sawing microtome technique. The slices were stained by methylene blue and basic fuchsin and studied with a light microscope (Zeiss, Gottingen-Germany). The light microscopy assessment consisted of a complete morphological description of the tissue response to the implants with different surface topography. Discriminating cell type was achieved by staining the samples and related cells shape differences. Osteoblasts can be in two states; (a) active, forming bone matrix; (b) resting or bone-maintaining. Those that make collagen, glycoproteins and proteoglycans of bone the matrix and control the deposition of mineral crystals on the fibrils. Osteoblast becomes an osteocyte by forming a matrix around itself and is buried. Lacunae empty of osteocytes indicate dead bone. Osteoclast, a large and multinucleated cell, with a pale acidophilic cytoplasm lies on the surface of bone, often an eaten-out hollow-Howship,s lacuna. Macrophages, are irregularly shaped cells that participate in phagocytosis.

3. RESULTS

Etch depth per pulse variation as a function of laser fluence which is shown in Figure 1 can be calculated from Equation 2.

$$X = \alpha^{-1} \ln (F/F_t) \quad (2)$$

In Equation 1, X is etch depth, α shows absorption coefficient and F_t is threshold fluence. Interaction

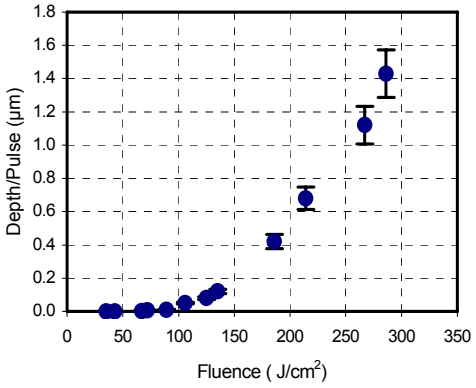

Figure 1. Variation of etch depth as function of fluence.

of laser radiation with metal surface can be divided into three distinct regions.

Zone I clearly indicates that there is no morphological changes below 72 Jcm^{-2} but beyond that where zone II commences, the melting gradually occurs and continues up to 145 Jcm^{-2}. It is however, important to notice from a metallurgical point of view that melting initially begins from possible inclusions due to high temperature rise and gradually joining these molten centers together, hence producing a molten pool as seen in Figure 2. Zone III begins with thermal ablation of Ti6Al4V at ≥ 145 Jcm^{-2}. However, the plasma formation took place slowly at higher fluences and became stronger as this parameter increased. Some cracks were observed at the laser treated sites. These cracks are probably due to residual mechanical stress originating from the temperature gradient at the end of pulse. Also, other factors like surface composition, solubility degree of alloys and base metal, thermal diffusion and heating/cooling rates may have specific roles in crack formation.

Relations between surface temperature and laser fluence can be shown as Equation 3 indicating non-adiabatic condition, governing the experiment.

$$T_f - T_i = (1 - R)\, F / \{\rho c\, (4k\tau_p)^{0.5}\} \quad (3)$$

Where [17]:

T_f, T_i = Final and initial surface temperature (°c).
R = Surface reflection (0.6)
C = Specific heat capacity (0.52 $Jg^{-1}°c^{-1}$)
ρ = Density (4.51 gcm^{-3})
k = Diffusivity coefficient (0.07 cm^2s^{-1})
τ_p = Pulse width (200 μs)

Figure 3 shows the variation of Ti6Al4V surface temperature as a function of fluence. Considering the melting and vaporization point of Ti6Al4V (1668ºC and 3280ºC, respectively) and the related fluence which can be calculated from Equation 2, the treatment fluence should be chosen between 72 Jcm^{-2} and 145 Jcm^{-2}. The comparison between two morphologically different areas i.e. laser treated and untreated is shown in Figure 4. As it is observed the inclusions have disappeared and the scratches due to machining and polishing are sealed due to direct laser heating surface. The experimental results from EDXA test are given in Figure 5.

Maximum reduction of vanadium in the alloy chemical composition seems to occur at 140 Jcm^{-2} which is thought to be due to element ratio offset caused by different melting temperatures at higher fluences. Thus, it is predicted that a better cell adhesion and growth will occur in the laser treated specimen at above value as surface toxicity is reduced. Surface hardness analysis shows an increase of surface hardness with laser fluence increase. 50 % improvement of surface hardness in 140 Jcm^{-2} is clearly observable in comparison with untreated

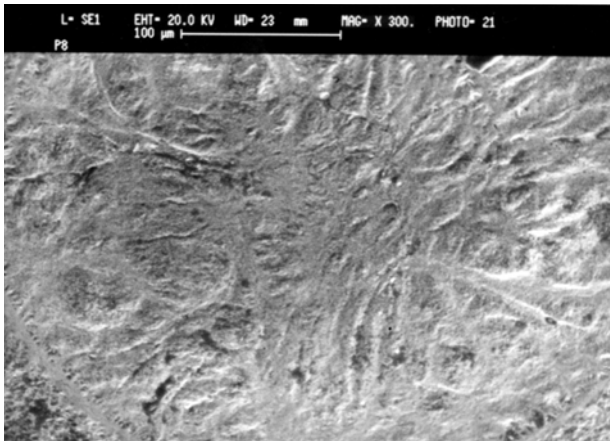

(a)

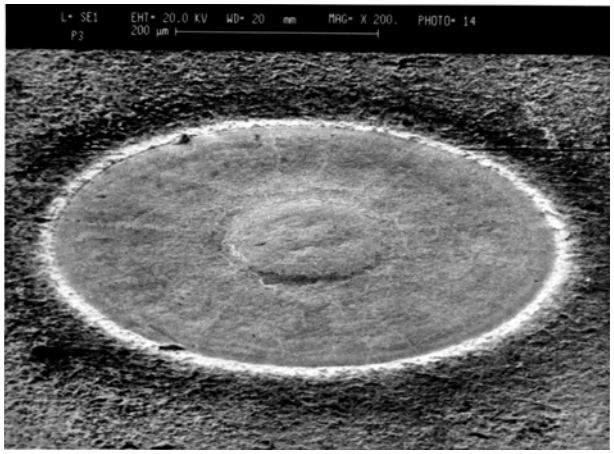

(b)

Figure 2. Ti6Al4V surface morphology (a) F = 90 Jcm^{-2} (b) F = 210 Jcm^{-2}.

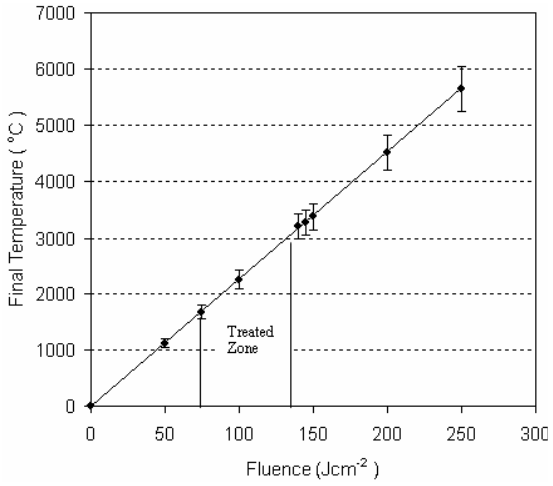

Figure 3. Variation of surface temperature with fluence.

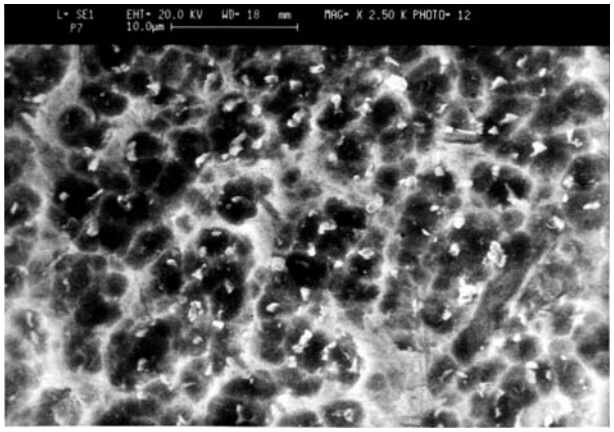

(a)

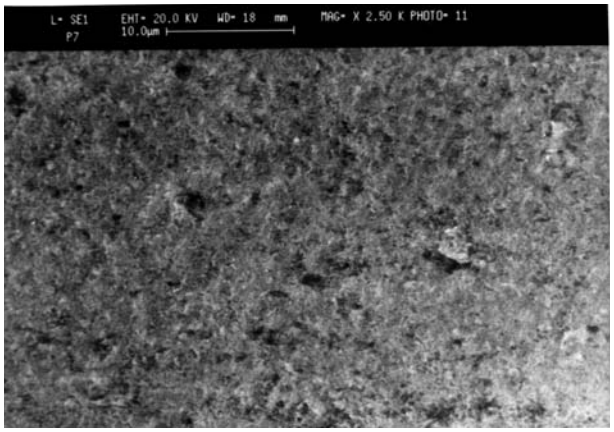

(b)

Figure 4. Ti6Al4V surface morphology (a) Untreated (b) Laser treated at 140 Jcm^{-2}.

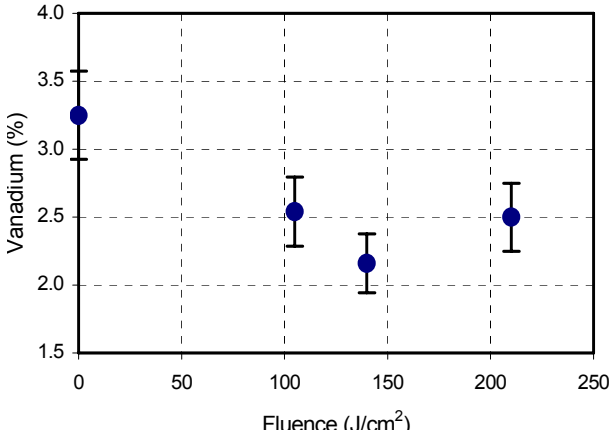

Figure 5. Changes of vanadium percent at the alloy surface as a function of fluence.

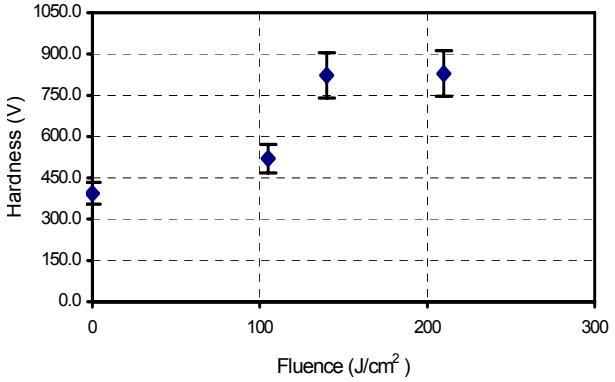

Figure 6. Variation of surface hardness versus fluence.

specimen, as it is shown in Figure 6.

This can be due to the fact that laser radiation has caused a smoother surface. Generally, change in surface hardness shows a microstructure modification in metallic bonds. The experimental results obtained from a corrosion test is given in Figure 7. This figure shows typical Tofel polarization curves for untreated and laser treated Ti6Al4V in Hank's salt balanced physiological solution.

The comparison of these curves indicates a few important points which are as follows: the corrosion rate for laser treated specimen reduced to 0.46 mpy at 140 Jcm^{-2} whose untreated value is 1.77 mpy. Also corrosion potential varied from-

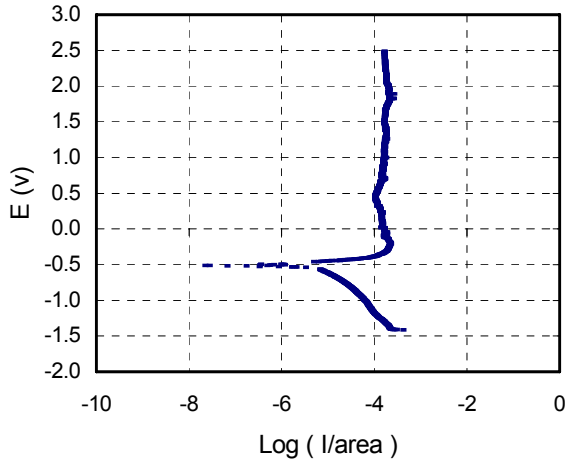

(a)

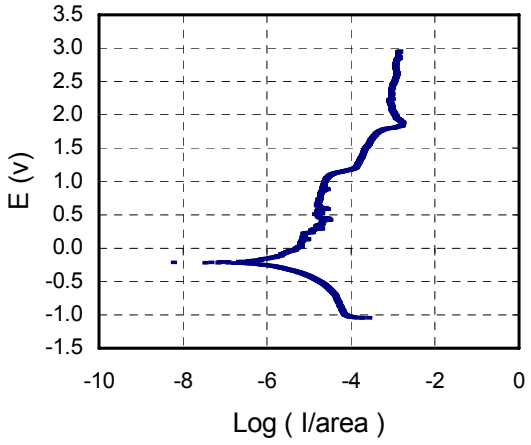

(b)

Figure 7. Corrosion test (a) Untreated (b) Laser treated at 140 Jcm^{-2}.

0.51 V to-0.21 V after the treatment process at 140 Jcm^{-2}. This implies that treated specimen release hydrogen easier and act as an electron donor to electrolyte. The corrosion current, also, decreased from 2.54 μAcm^{-2} to 0.66 μAcm^{-2} after surface treatment, which means a better corrosion resistance. The passive region is directly affected by laser radiation and changes from 0.85-1.25 V to 0.1-1.25 V in value. Thus a more noble metal is achieved. Increase of corrosion resistance probably means that most inclusions at the surface have been dissolved in the structure due to melting or alternatively, they are covered by molten material. In other words, since Ti has bio inert property, the increase in percentage of Ti distribution over the surface can be another explanation for a better corrosion resistance.

Change in surface wettability was studied by contact angle measurement for both untreated and laser treated specimens at, 100 Jcm^{-2} and 140 Jcm^{-2} whose results are shown in Figure 8. A smoother surface was achieved by laser radiation at 140 Jcm^{-2} which may affect the degree of wettability. It is, however, important to note that a smoother surface and enhanced oxygen content, which depends on oxide layer thickness, can both help to reduce the contact angle. This is so because the surfaces with higher concentration of oxygen atoms and more incorporation of oxygen-base polar functionalities of surface exhibit higher wettability (i.e. lower contact angle) hence an improvement of biocompatibility, though some believe that, hydrophilicity alone is an inadequate promoter of cell adhesion and retention [18]. As a result, it is emphasized that a better cell adhesion can be obtained for the specimen with apparently higher surface energy, rather than higher surface roughness.

According to primary melting centers topology, the surface roughness increased slightly at 100 Jcm^{-2}. Thus an increase of contact angle occurs from 70º to 80º indicating a lower degree of

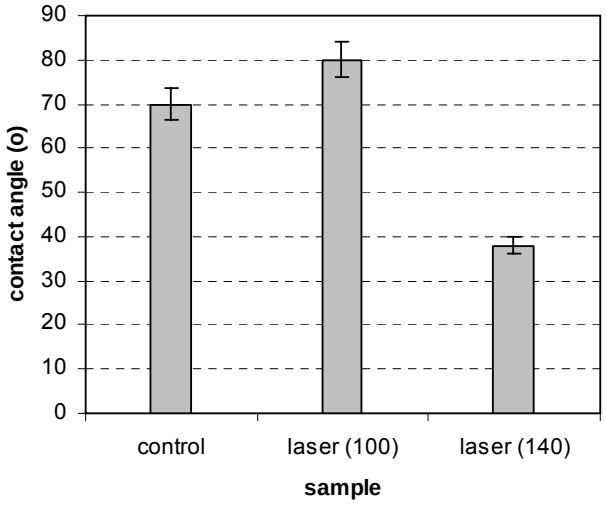

Figure 8. Contact angle measurement for different samples.

TABLE 1. Bone Cell's Spread Over the Implanted Specimens Surface.

Row	Fluence (Jcm^{-2})	Spread Cell Area (μm^2)
1	0	316 ± 10
2	100	352 ± 6
3	140	488 ± 8

wettability. Following the laser treatment at 140 Jcm^{-2} the contact angle reduced to 37º still giving a more acceptable hydrophilicity. The experimental results of biocompatibility and bone cell growth are given in Table 1. As can be seen bone cell spread over the specimen surface for laser treated or untreated is related to laser fluence. This spreading over the surface was measured by Image J program software (IJP).

The SEM analysis of attached cells morphology indicates that the density of cell network is directly dependent on the laser beam fluence. The smooth surface at 140 Jcm^{-2} not only caused a dense cell network but also resulted in a wider area covered by a single cell spreading. Density of the network originated from monolayer attachments (cell-surface) changes to multilayer (cell-surface and cell-cell). As is seen in Figure 9, no specific directional spread of attached cells was achieved in laser treated specimens.

Enzyme detachment tests indicated that much more cell attachment (1.2×10^5) at 140 Jcm^{-2} for laser treated specimen compared with 0.7×10^5 and 0.4×10^5 for laser treated at 100 Jcm^{-2} and untreated specimen respectively. Figure 10 shows the number of attached cells to the surface as a function of time.

When the implants were retrieved, no inflammatory reaction was observed inside or around the implants. Mineralized matrix deposition and bone cells were observed on the surface of the implants which are formed during the eight month implantation. Mineralized matrix deposition was found on all sides of the implants and bone formation was characterized by the occurrence of osteocytes embedded in a mineralized matrix.

Qualitative evaluation of macrophage, osteoblast, osteoclast, polymorpho nuclear leukocytes (PMN), giant cells, fibroblast, lymphosite and healing was carried out during pathology tests (Table 2). The symbols given in Table 2, indicate the presence of cells (+), high (++), very high (+++) and lack of cells (-) respectively.

No PMN, giant cells and osteoclast were seen in the laser treated sample at 140 Jcm^{-2}. Also tissue healing was better conducted near the mentioned implant rather than all other evaluated specimens. Fibroblast and osteoblast cells were also numerous in qualitative scales for 140Jcm^{-2} case Figure 11.

4. DISCUSSION

When considering materials for application of orthopaedic implants, it is important to consider a number of factors such as surface hardness, corrosion resistance, biocompatibility and surface wettability. However, since laser surface processing of materials is an area of considerable importance, technological parameters of radiation must be carefully optimized in order to obtain a unique surface structure. It has been found that the key to improving modification efficiency and the quality is not only the laser power dependent but also depends on the spatial and temporal profile of the laser beam. All the phenomena occurring in this area in regard to the interaction of laser beam-material, including energy deposition, melting, evaporation and ablation depend on optical parameters (energy density, pulse duration, pulse number) as well as on physico-chemical and optical properties of material.

In the present study, laser-material interaction can simply be considered as a non-adiabatic thermal process, since thermal evaporation is the dominant mechanism in the system where surface melting is observed ie. at about 70 Jcm^{-2}. So selecting proper energy density for surface treatment, has direct influence on surface hardness,

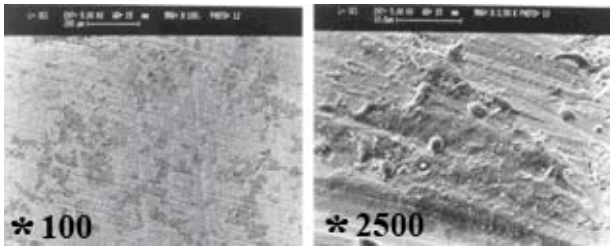

(a)

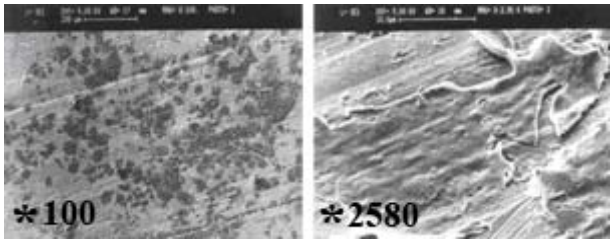

(b)

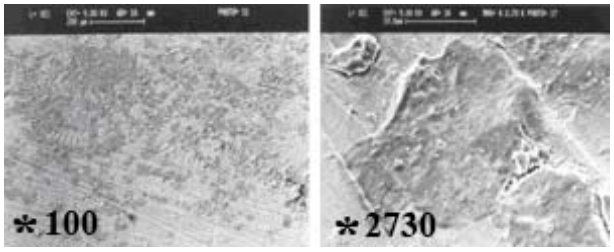

(c)

Figure 9. Scanning electron micrographs of attached cells on the surface for (a) Untreated (b) Treated at 100 Jcm^{-2} (c) Treated at 140 Jcm^{-2}.

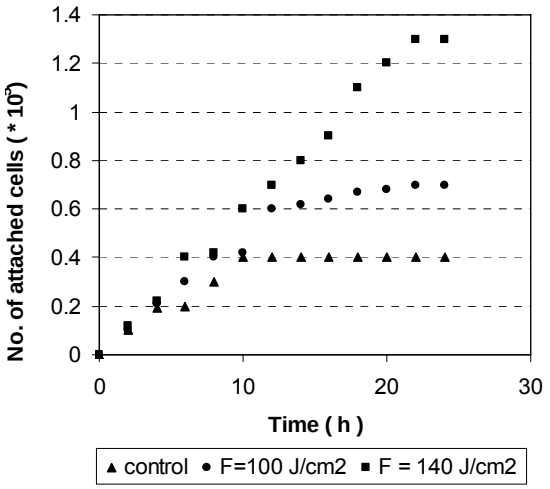

Figure 10. Number of attached cells on the surface of sample as a function of time.

corrosion resistance, surface composition and surface wettability of Ti6Al4V. According to these study results, surface laser treatment at 140 Jcm^{-2} and 10 pulse brought an acceptable and positive effect on surface property improvement.

Reduction of Titanium-Vanadium difference, in the total amount of alloy composition is one of the most valuable results of this research. This event causes an increase of cell growth and better cell adhesion to the implanted surface. However, it is worth noting that the lower toxicity due to an increase in Ti-V difference has a great impact on the implant biocompatibility. The present research, showed that the surface laser treatment at 140 Jcm^{-2} increases the surface hardness by 50 percent compared with untreated surfaces. This implies a better abrasion resistant achievement due to micro structural modifications of metallic bonds. Another important result of this study was an increase of corrosion resistance. The corrosion rate decreased by 74 percent due to surface inclusion removal after laser treatment. As a result of which, extending the passivity region by 60 percent making this alloy much more noble after laser treatment.

In terms of biocompatibility, there was a decrease of contact angle due to the surface treatment process which can cause more cell adhesion to the surface and subsequently result in better biocompatibility. According to the results, two regions in Figure 1 worth to discus. First, from 0 to 100 Jcm^{-2} where the measured surface contact angle was increased with the surface roughness due to appearance of surface melting. Secondly, from 100 Jcm^{-2} to 140 Jcm^{-2} where the contact angle was decreased by about 50 percent when the surface became smoother.

In addition to surface morphology, the properties of implant materials affect cellular behavior such as wettability. The wettability of the surface plays an important role with respect to protein adsorption, cell attachment and spreading. It is known that surfaces with high surface free energy are to be more adhesive than those with a

TABLE 2. Qualitative Evaluation of Histology Results of Bone Tissue Around the Implants with Different Surface Morphology.

Sample / Cell	100 Jcm^{-2}	140 Jcm^{-2}	untreated
Fibroblast	+++	+++	++
Osteoblast	++	+++	+
Giant cell	-	-	-
Osteoclast	-	-	+
PMN	+	-	+
Lymphocyte	+++	++	++
Macrophage	+++	++	++
Healing	+	++	+

low surface free energy. The surface tension at 140 Jcm^{-2} was about 1.5 times greater than the untreated sample. It is also worth noting that all the samples were treated in ambient condition and were steam sterilized which would have a great influence on the surface composition of Ti especially in TiO_2 formation. It is proved that the samples irradiated by laser during treatment can lead to oxygen diffusion through the molten materials and, thus, oxidation of the titanium [19].

Bone cell adhesion to surface depends directly on how easy the collagen or non collagen protein (osteocalcine, osteonectin, syalo protein, glycol protein, …) reach the surface as they play an important role on the adhesion process. The focal point in laser treated surfaces at 140 Jcm^{-2} is approximately 10 nm which is convenient for bone cells to get close to, be activated and attach to the surface in order to form an extra cellular matrix (ECM). In this state, bone cells will spread over the smooth surface much more easily and fluently. It seems, however, that the laser treated surface did not regulate the cell's shape similar to other investigations [20,21]. Due to laser surface treatment at 140 Jcm^{-2}, and a smooth surface, the bone cells come close to the surface at the distance of about10 nm. A distance which is called focal distance, in this case about 10 nm is the most convenient value for the cell proteins to be activated and begin attaching to the surface and form the extra cellular matrix. The first important step in surface bone formation is the amount of cells which find the capability to attach the surface. Following the above steps, the other cells in the next layer attach easier to the implanted specimen Therefore, in 140 Jcm^{-2} more cell attachment to the surface takes place and hence dense and multilayered adhesion sites are formed.

5. CONCLUSION

It is concluded from preliminary in vivo tests that Nd: YAG laser can induce a desirable surface modification on Ti6Al4V alloy. In order to achieve the best experimental results, the irradiation process must be optimized in terms of optical parameters. The SEM, corrosion test, EDXA, contact angle measurement together with the in vivo experiment confirm that a noble and biocompatible Ti alloy with better physio-chemical properties can be obtained under suitable physical conditions. Finally, we believe that more investigations are needed to further clarify the fundamentals of cell adhesivity on smooth surfaces and cell attachment onto rough surfaces.

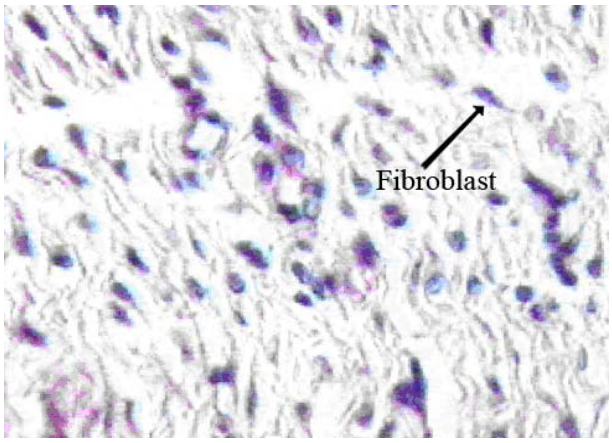

(a)

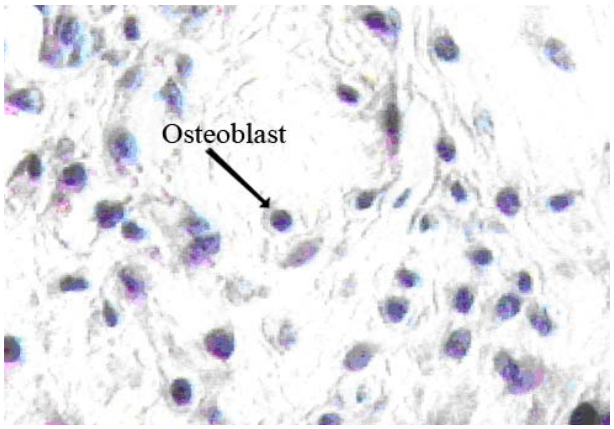

(b)

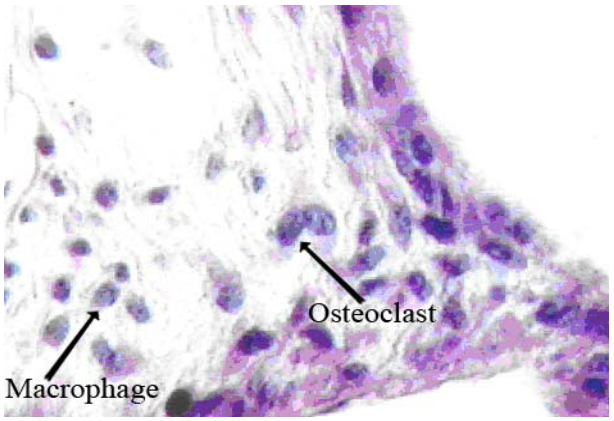

(c)

Figure 11. Light microscopy evaluation of bone tissue for: (a) Laser treated at 140 Jcm^{-2}, (b) 100 Jcm^{-2} Untreated.

6. REFRENCES

1. Adell, R., Lekholm, U. and Rokler, B., "A 15-Year Study of Osseointegrated Implants in the Treatment of the Edentulous Jaw", ***Int. J. oral Surg***., Vol. 10, No. 6, (1981), 387-416.
2. Long, M. and Rock, H. J., "Titanium Alloys in Total Joint Replacement, A Material Science Prespective (Review)", ***Biomaterials***, Vol. 19, (1999), 1621-1639.
3. Rondelli, G. and Vicenti, B., "Localized corrosion Behaviour in Simulated Human Body Fluids of Commercial Ni-Ti Orthodentic Wire", ***Biomaterioals***, Vol. 20, (2001), 785-792.
4. Feng, B., Weng, J., Yang, B. C., Qu, S. X. and Zhang, X. D., "Characteristic of Surface Oxide Films on Titanium and Adhesion of Osteoblast", ***Biomaterials***, Vol. 24, (2003), 4643-4670.
5. Satsangi, A., Satsangi, N. and Glover, R., "Osteoblast Response to Phospholipid Modified Titanium Surface", ***Biomaterials***, Vol. 24, (2004), 4585-4589.
6. Ronald, H. J., Lyngstadas, S. P. and Ellingsen, J. E., "Analysis the Optimal Value for Titanium Implant Roughness in Bone Attachment Using a Tensile Test", ***Biomaterials***, Vol. 24, (2003), 4559-4564.
7. Anselme, K., Bigerelle, M. And Iost, A., "Effect of Grooved Titanium Sabstrum on Human Osteoblastic Cell Growth", ***J. Biomed. Mater. Res***., Vol. 60, (2002), 529-540.
8. Links, J., Boyan, B. and Blanchard, C., "Response Of MG63 Osteoblast-Like Cells to Titanium and Titanium Alloys Depends on Surface Roughness and Composition", ***Biomaterials,*** Vol. 19, (2002), 2219-2232
9. Beraceras, I., Alava, I., Onate, J. I. and Maezto, M. A., "Improved Osseointegration in Ion Implantation-Treated Dental Implants", ***Surf. Coat. Tech***., Vol. 158, (2002), 28-36.
10. Tian, Y. S., Chen, C. Z., Yue, T. M. and Wang, Z. L., "Study on Microstructures and Mechanical Properties of in-Situ Formed Multiphase Coating by Laser Cladding of Titanium Alloy with Silicon and Graphite Powder", ***China. J. Laser***, Vol. 31, (2004), 1-12.
11. Khor, K. A., Vreeling, A., Dong, Z. L. and Cheang, P., "Laser Treatment of Plasma Sprayed HA Coatings", ***Mater. Sci. Eng***., Vol. 266, No. A, (1999), 1-8.
12. Tritca, M. S., Tarasenko, V., Gakovic, B. and Fedenev, A., "Surface Modification of Tin Coating by Pulsed the CO_2 and Xecl Lasers", ***Appl. Sur. Sci.***, Vol. 252, (2005), 474-482.
13. Hollander, D., Walter, M., Wirtz, T., Paar, O. and Eril, H., "Structural Mechanical and *in vitro* Characterization of Individually Structured Ti6Al4V Produced by Direct Laser Forming", ***Biomaterials***, Vol. 27, (2005), 955-963.
14. Peyer, P., Scherpereel, X., Berthe, L., Carboni, C., Fabbro, R. and Lemaitre, C., "Surface Modification Induced in 316L Steel by Laser Peening and Shot-Peening: Influence of Pitting Corrosion", ***Mat. Sci. Eng***., Vol. 280, (2000), 294-302.
15. Tritca, S., Gakovic, M., Nenadovic, M. and Mitrovic, M., "Surface Modification of Stainless Steel by Tea Co_2

Laser", ***Appl. Sur. Sci***., Vol. 177, (2001), 48-57.
16. Wieland, M., Textor, M., Spencer, N. D. and Brunette, D. M., "Wavelength-Roughness: A Quantitative Approach to Characterizing the Topography of Rough Titanium Surfaces", ***Int. J. Oral. Maxilloface Impl***., Vol. 16, No. 2, (2001), 163-181.
17. Ifflander, R., "Solid State Lasers for Material Processing", ***Springer Series in Optical Sciences***, Chap. 3, Berlin, (2001), 257-328.
18. Baier, R. E., Meyer, A. E., Natiella, J. R., Natiella., R. R. and Carter, J. M., "Degradative Effects of Conventional Steam Sterilization on Biomaterial Surfaces", ***J. Biomed. Mater. Res***., Vol. 18, (1984), 337-355.
19. Ronold, H. J., Lyngstadaas, S. P. and Ellingsen., J. E., "A Study on the Effect of Dual Blasting with Tio_2 on Titanium Implant Surfaces on Functional Attachment In Bone", ***J. Biomed. Mater. Res***., Vol. 67, No. A, (2003), 524-530.
20. Hao, L., Lawerence, J. and Li, L., "The Wettability Modification of Bio-Grade Stainless Steel in Contact with Simulated Physiological Liquids by the Means of Laser Irradiation", ***Appl. Sur. Sci***., Vol. 247, (2005), 453-457.
21. Hao, L., Lawerence, J. and Li, L., "Manipulation of the Osteoblast Response to a Ti6Al4V Titanium Alloy Using a High Power Diode Laser", ***Appl. Sur. Sci***., Vol. 247, (2005), 602-606.